HHS Public Access

Author manuscript

Biofabrication. Author manuscript; available in PMC 2019 March 28.

Published in final edited form as:

Biofabrication. ; 10(3): 035004. doi:10.1088/1758-5090/aaafbc.

Matrix Stiffness and Tumor-Associated Macrophages Modulate Epithelial to Mesenchymal Transition of Human Adenocarcinoma Cells

Marta Alonso-Nocelo[1], **Theresa M. Raimondo**[2,3], **Kyle H. Vining**[2,3], **Rafael López-López**[1], **Maria de la Fuente**[1,*], and **David J. Mooney**[2,3,*]

[1]Translational Medical Oncology Group, Health Research Institute of Santiago de Compostela (IDIS), SERGAS, CIBERONC, 15706 Santiago de Compostela, Spain

[2]John A. Paulson School of Engineering and Applied Sciences, Harvard University, Cambridge, MA 02138, USA

[3]Wyss Institute for Biologically Inspired Engineering, Harvard University, Boston, MA 02115, USA

Abstract

The tumor microenvironment (TME) is gaining increasing attention in oncology, as it is recognized to be functionally important during tumor development and progression. Tumors are heterogeneous tissues that, in addition to tumor cells, contain tumor-associated cell types such as immune cells, fibroblasts, and endothelial cells. These other cells, together with the specific extracellular matrix (ECM), create a permissive environment for tumor growth. While the influence of tumor infiltrating cells and mechanical properties of the ECM in tumor invasion and progression have been studied separately, their interaction within the complex TME and the epithelial-to-mesenchymal transition (EMT) is still unclear. In this work, we develop a 3D co-culture model of lung adenocarcinoma cells and macrophages in an interpenetrating network hydrogel, to investigate the influence of the macrophage phenotype and ECM stiffness in the induction of EMT. Rising ECM stiffness increases both tumor cell proliferation and invasiveness. The presence of tumor-associated macrophages and the ECM stiffness jointly contribute to an invasive phenotype, and modulate the expression of key EMT-related markers. Overall, these findings support the utility of in vitro 3D cancer models that allow one to study interactions among key components of the TME.

Keywords

hydrogels; tumor microenvironment; macrophages; stiffness; EMT

[*]Corresponding Authors: Maria de la Fuente Ph.D. (maria.fuente.freire@gmail.com); David James Mooney Ph.D. (mooneyd@harvard.edu).

Author Contributions

MAN, RLL, MF and DJM developed the study concept and designed the experiments. MAN, TMR and KHV conducted experiments and analyzed data. MAN, TMR, KHV, MF and DJM wrote and edited the manuscript.

Conflict of Interests

The authors declare that there is no conflict of interests regarding the publication of this paper.

1. Introduction

Although EMT is believed to be a fundamental step in cancer cell metastasis, only a limited number of studies have considered the complexity of the tumor microenvironment (TME) in this process. The TME is characterized by an intricate and sophisticated network of interactions among different cellular components and the extracellular matrix (ECM), all of which contribute to the microenvironmental regulation of tumor progression and metastasis [1,2]. It consists of ECM, stromal cells such as fibroblasts, infiltrating immune cells and the vasculature [3–6]. The ECM is no longer considered just a supportive structure, but is now recognized as an essential dynamic compartment, hosting multiple biochemical and mechanical signals that modulate tumor progression [6,7]. Indeed, ECM remodeling and stiffening of the TME strongly correlate with tumor progression [8,9]. ECM stiffness enhances cell growth and survival and promotes migration, affecting the malignant transition of cells and the formation of metastasis [6,10–12]. Both tumor and stromal cells can affect the ECM structure and composition [13]. Furthermore, infiltrated immune cells such as macrophages produce enzymes and cytokines that lead to alterations in the ECM architecture, promote fibrosis and increase matrix stiffness [14,15].

Among the different immune cells that can be found in the TME, tumor-associated macrophages (TAMs) are attracting a great deal of interest as they can represent up to 50% of the tumor mass [16]. As the major inflammatory component of the stroma, they constitute a driving force in proliferation, matrix remodeling, metastasis, and suppression of adaptive immunity in various tumors [17–20]. The tumor milieu itself strongly influences the recruitment of normal macrophages (M0) and shapes several of their features, as these cells display remarkable plasticity and change their physiology in response to microenvironmental cues [21–24]. TAMs can exert distinct influences in cancer, depending on their activation state. Classically activated macrophages, termed M1 or pro-inflammatory macrophages, produce effector molecules such as reactive oxygen intermediates, reactive nitrogen intermediates, and TNFα, to limit tumor growth. M2 or alternatively activated macrophages, in contrast, promote tumor growth and metastasis by secretion of matrix-degrading enzymes, angiogenic factors, and immunosuppressive cytokines and chemokines [25]. It is now appreciated that M2 macrophages can be further divided into subsets, specifically M2a, M2b, M2c and M2d based on their different gene expression profiles. For instance, M2a macrophages are involved in Th2 type immune response e.g. against parasites; whereas M2c are involved in tissue repair and remodeling [26,27].

In vitro 3D models have facilitated progress in the understanding of the different stages of cancer progression [28,29], and allow one to more readily focus on the role of specific features than is often possible using in vivo models. Several types of biomaterials, in particular hydrogels, which have high tissue-like water content and tunable physical and mechanical properties, have shown the potential to mimic native ECM and serve as a tumor matrix [30,31]. They can be specifically designed to mimic stiffness and other mechanical properties of tumors in order to understand their impact on tumor invasiveness and metastasis [32–34]. Protein components of the ECM such as collagen, fibrin, laminin, or elastin, as well as mixtures of these materials or other hybrid protein-based matrices such as Matrigel, are widely used as cell-culture substrates due to their inherent resemblance to the

natural ECM and complex signaling capabilities [35]. Cramer et al. used collagen I and Matrigel to evaluate how ECM composition and rigidity affect the invasive behavior and motility of pancreatic ductal adenocarcinoma cells [36]. Similarly, Nguyen-Ngoc et al. analyzed the effect of ECM composition in the migratory pattern and dissemination of both tumor and normal murine mammary epithelium [37]. However, gels based solely on these materials do not allow one to decouple changes in matrix stiffness from changes in composition and 3D architecture [12,38]. In addition, studies exploring co-culture of tumor and tumor-infiltrating cells have typically been based on transwell assays [39–43], failing to reproduce a physiological relevant environment for cell-cell and cell-ECM interaction and crosstalk. To the best of our knowledge, 3D models considering the interactions between tumor and immune infiltrating cells, with control over the ECM stiffness, have not been previously developed.

This study was performed to specifically evaluate the contributions of alternatively activated macrophages and the ECM stiffness on the metastatic potential of co-cultured tumor cells, and the promotion of an epithelial-to-mesenchymal transition (EMT). A previously characterized hydrogel system, based on an interpenetrating network (IPN) of alginate and Matrigel that allows one to vary ECM stiffness independently of composition and 3D architecture [44], was used to investigate how mechanical signals crosstalk with co-cultured macrophages to modulate invasion and EMT in lung adenocarcinoma cancer cells. As polymer concentration is constant in the system, the average pore size is similar for all the IPNs, therefore not affecting diffusion. To study the influence of macrophages on the tumor cells, we have used THP-1 differentiated macrophages, which demonstrate similar expression profiles as polarized primary macrophages [45].

2. Methods

2.1. Cell culture

The lung adenocarcinoma cell line A549 (ATCC® CCL-185™) was grown in DMEM Dulbecco’s modified Eagle’s Medium (GIBCO, Spain). The human monocytic leukemia cell line THP-1 (ATCC® TIB-202™) was grown in RPMI-1640 (Sigma). Both media were supplemented with 10% heat-inactivated fetal bovine serum (HI-FBS) (GIBCO) and 1% penicillin-streptomycin (GIBCO). RPMI was also supplemented with HEPES (10 mM), sodium pyruvate (110 mg/L) and 2-mercaptoethanol (0.05 mM). Cells were cultured in a standard humidified incubator at 37°C in a 5% CO2 atmosphere.

2.2. Interpenetrating Networks (IPNs) formation and characterization

All IPNs in this study were prepared from a solution of 4.4 mg/mL Matrigel (Corning) and a solution of 5 mg/mL alginate, in a total volume of 0.5 mL, as previously described in [44]. Briefly, alginate was initially dialyzed, purified and lyophilized (see Supplementary information). For each gel, alginate was first reconstituted at 2.5% in Dulbecco’s modified Eagle’s medium (DMEM) and then delivered into a 1.5 ml tube and put on ice. A final 0.5 wt% alginate was selected in order to allow appropriate mixing of the stock alginate solution with the viscous Matrigel solution, the cells and calcium sulfate slurry.

On the other hand, cells were trypsinized, counted, diluted to the appropriate concentration and then placed on ice. Cells were encapsulated as monocultures at a cell density of 2×10^5 cells/ml and as co-cultures at 2×10^5 and 4×10^5 cells/ml for tumor cells and macrophages, respectively. After the alginate had cooled, Matrigel, also on ice, was added to the alginate, and mixed ~30–60 times with a pipette, being careful not to generate bubbles. The mixture was kept on ice before IPN formation.

Next, different concentrations of Ca2+ were used to crosslink the alginate. Previous rheology studies to characterize the mechanical properties of the IPNs [42] showed that by modulating the amount of calcium, the storage modulus of the IPNs at 1Hz can be tuned from 30 to 310 Pa while maintaining a constant polymer composition. Therefore, a solution containing calcium sulphate was prepared. Calcium sulphate was first dissolved in water at 1.22 M and then autoclaved. This solution was then diluted ten-fold in serum-free DMEM just before the experiment. For each gel, 100 μl of serum-free DMEM containing the appropriate amount of the calcium sulphate slurry (4.88, 9.76 and 19.5 mM) was added to a 1 ml Luer lock syringe (Cole-Parmer) and kept on ice.

Once all three components had been individually prepared, the gels were formed one by one. First, cells were pipetted into the Matrigel/alginate tube and mixed ~60 times with a pipette. Then the cell/Matrigel/alginate solution was transferred with a pipette into a cooled 1 ml Luer lock syringe. The syringe with the calcium sulphate solution was then shaken to mix the calcium sulphate evenly, and then the two syringes were coupled together with a female–female Luer lock (Cole Palmer), taking care not to introduce bubbles or air into the mixture. Finally, the two solutions were mixed rapidly together with three pumps of the syringe handles and instantly deposited into a well in a plate that had been pre-coated with Matrigel. The plate was then placed in an incubator, and the IPNs were allowed to gel for 30–50 min before media was added to the wells.

2.3. Image analysis of cell clusters

Both cross-sectional area and invasiveness of adenocarcinoma lung cell clusters, seeded in IPNs as mono-cultures, were analyzed every other day for each condition. Differential interference contrast (DIC) images at 10X of at least 6 randomly selected clusters were taken. Then, using a semi-automated algorithm in ImageJ (NIH), the image was thresholded, highlighting the boundaries between the clusters and the matrix, and the area of each cluster was calculated. In some cases of highly invasive clusters at high stiffness, the margin between the cell cluster and matrix had to be manually drawn to avoid underestimation of cluster size. At least 4 independent gels were analyzed for each data point.

2.4. Staining of primary lung tumor tissue

Human lung adenocarcinoma samples from the Pathology Department (University Clinical Hospital of Santiago de Compostela) were selected by the pathologist for comparison to the in vitro findings of this study. Paraffin sections (4 μm) of two independent specimens were processed and stained for hematoxylin and eosin (H&E). Illustrative photos were taken from standard H&E stained tissue slides.

2.5. Conditioned Media Assays in IPN mono-cultures

Conditioned media (CM) was collected from cultures of macrophages polarized to different phenotypes (M0, M1, M2a and M2c). Macrophages were washed with PBS (2x), and cultured for 18 h in RPMI 1% HI-FBS (without IFNγ/LPS or cytokines) before collection. CM was then centrifuged (500 RCF, 6 min, 4°C) to remove cell debris and stored in aliquots at −20°C. Then, media were concentrated using Amicon Ultra 3K filters (Millipore, Billerica, MA). Concentrated CM from macrophages was re-diluted (1:8) in complete RPMI medium (10% FBS). The number of macrophages that conditioned the media was adjusted to be equivalent to 2 times the number of tumor cells seeded in the gels. Macrophages phenotype was evaluated before and after collecting the CM (Supplementary Methods and Fig S2).

Tumor cells were encapsulated in IPNs and cultured for up to 6 days. CM from macrophages polarized to different states (M0, M1, M2a and M2c) or control medium were added on days 4 and 6. Cluster area and invasiveness of cells were monitored every other day for all the conditions. On day 6, cells were harvested from the IPNs for qPCR analysis.

2.6. IPN co-cultures of macrophages and tumor cells

Tumor cells and M0 or M2c macrophages were encapsulated into IPNs and co-cultured for 3 and 6 days. Macrophage phenotype was assessed before every experiment by flow cytometry Supplementary Information). Cluster area and invasiveness of the tumor cells were monitored every other day for all the conditions. On day 6, gels were fixed for OCT embedding. Moreover, cells were also harvested for FACS and qPCR analysis. Mono-cultures of tumor cells and macrophages (M0 or M2c macrophages) were used as controls.

2.7. Cell retrieval for gene expression and flow cytometry analyses

Once experiments were concluded, cells were retrieved from IPNs for RNA expression and flow cytometry analysis. For this purpose, media was first removed from the gels, and the gels were then placed directly in 5 ml of cooled PBS with 50 mM EDTA on ice. This mixture was pipetted and vortexed periodically to disassociate the gels. The mixture was then centrifuged (400 RCF, 6 min, 4°C) to separate the pellet of cells. For analysis of RNA expression, the cells were washed again with PBS, spun down, and the pellet was lysed using RNA extraction RLT buffer (RNeasy Kit, Qiagen). Alternatively, for flow cytometry, the cell pellet was treated with accutase stem pro for 15 minutes to break up any remaining adherent matrix or cell clusters and obtain a single cell suspension. Ultimately, the cells were stained for flow cytometry as described in the Supplementary Information.

2.8. Quantitative real time PCR

RNA extraction was performed using the RNeasy Micro and Mini kits (6 and 3 day samples respectively) (Qiagen). RNA was quantified using a NanoDrop ND1000 Spectrophotometer (Thermo Scientific). Reverse transcription was carried out with the iScript™ cDNA Synthesis kit (Bio Rad); 1000 ng of total RNA were used per sample. The expression profile of a panel of genes was assessed with the SsoAdvanced™ Universal SYBR® Green Supermix (Bio Rad), on a 96-well plate format and using a CFX96 real-time PCR detection

system (Bio-Rad) with 10 ng per well. Relative expression values were generated using ΔCt values normalized to GAPDH.

2.9. Preparation of gels for immunohistochemistry and immunofluorescence

For immunohistochemical staining, media was first removed from the gels and then gels were fixed with 4% paraformaldehyde in serum free DMEM at 37°C for 30 – 45 minutes. The gels were then washed 3 times in warmed PBS containing calcium (cPBS), and incubated overnight in 30% sucrose in cPBS at 4°C. Then the media was removed, the gels were embedded in OCT and frozen. Frozen gels were sectioned with a cryostat (Leica CM1950) to a thickness of 40 μm and stained for Vimentin, E-cadherin and PD-L1 following standard immunohistochemistry protocols (for antibodies, see Supplementary Table 2). Negative controls, where the secondary antibody is added but the primary antibody is not, were conducted to ensure specificity of all stains.

2.10. Statistical analysis

All of the experiments were conducted in triplicate and the statistical analyses were performed using Prism 6 (La Jolla, California). For multiple comparison, statistical significance was determined using ANOVA followed by the Dunnett post-test. Data are shown as mean ± SD. All of the data from the PCR quantitative assays are expressed as means ± standard error mean (SEM). Significant differences between only two groups were evaluated with the 2-tailed nonparametric unpaired Mann and Whitney t test. Statistical significance is indicated by asterisks (*$p < 0.05$; **$p< 0.01$; ***$p< 0.001$; ****$p< 0.0001$).

3. Results

3.1. Increased stiffness of IPNs enhances tumor cell growth and invasiveness

The effect of ECM stiffness on the phenotype of the encapsulated A549 lung adenocarcinoma cells was first evaluated using IPNs of different stiffness (30, 80 and 310 Pa). These values represent a range of physiological to lower-end pathological stiffness of the tumor stroma [8]. Proliferation, as measured by the area of cell clusters (cluster area), and invasiveness of the tumor cells into the ECM, as indicated by quantification of the circularity of the cell clusters (circularity) were monitored for up to 6 days. Both cluster area (Fig 1A) and invasiveness (Fig 1B) were found to increase over time in all conditions. However, at day 6 significant differences in both parameters were observed for cells encapsulated within IPNs of the highest modulus (310 Pa), as compared to those seeded in IPNs of the lowest modulus (30 Pa). When the cells were encapsulated within IPNs of the lowest modulus (30 Pa), initially single A549 cells formed organotypic glands, as indicated by defined round cell clusters. When stiffness of the matrix was increased, clusters exhibited an elongated form and cells significantly invaded the matrix (Fig 1C–D). Importantly, the phenotypes observed in IPNs of the highest modulus, representing the lower-end of tumor stroma stiffness range [46], closely resembled cells in the glands of invasive human lung adenocarcinomas (Fig 1E).

3.2. Conditioned medium (CM) from macrophages of different phenotypes modifies tumor cell growth in IPNs of high stiffness

The effect of conditioned media obtained from different macrophage subtypes on the proliferation and invasiveness of A549 cells was subsequently investigated. Monocytes were differentiated into macrophages and then polarized to the M1, M2a, and M2c states; or left unstimulated (M0) (Supplementary Fig S1). Cells encapsulated within IPNs of stiffness 30 and 310 Pa were treated on days 2 and 4 with control or conditioned media obtained from macrophages of different subtypes (Fig 2). At the lowest stiffness (30 Pa), tumor cells responded differently in terms of proliferation (cluster area), following treatment with M0 and M2c conditioned media compared to control medium (Fig 2A). Regarding invasiveness (cluster circularity), cells showed a similar profile irrespective of the type of conditioned medium (Fig 2B). In IPNs with high stiffness (310 Pa), cluster area significantly increased in cells treated with conditioned medium from M2c macrophages compared to control medium. Conditioned media from M0 macrophages significantly inhibited tumor cell cluster proliferation (Fig 2C). Accordingly, the circularity of cell clusters treated with M0 conditioned medium was higher, but not significantly, as compared to the control (Fig 2D).

3.3. Higher stiffness maintains tumorigenic phenotype in the presence of M2c macrophage CM, by increasing expression of genes associated with EMT

Next, tumor cells growing in IPNs that were treated with M0 or M2c macrophage-conditioned media were harvested after 6 days in order to perform qPCR analysis. Relative expression of EMT-related genes was then analyzed (Figure 3). In IPNs of lower modulus (30 Pa), tumor cells showed a similar gene expression profile irrespective of the conditioned medium with which they were treated (Fig 3A). In contrast, in high stiffness IPNs (310 Pa), gene expression was strongly influenced in cells treated with conditioned media collected from M2c macrophages. The expression of *CDH2, MYC* and *TWIST1* was significantly increased in relation to cells treated with conditioned media from M0 macrophages (Fig 3B).

3.4. Co-culture with tumor cells induces the polarization of M0 macrophages towards a M2 phenotype in IPN co-cultures

To explore the potential interplay between tumor cells and macrophages, monocytes were differentiated to M0 and M2c macrophages (CD163−/CD45+ and CD163+/CD45+, respectively) and co-cultured with tumor cells in IPNs of low (30 Pa) and high (310 Pa) stiffness (Fig 4). The influence of tumor cell co-culture (CC) and matrix stiffness on the phenotype of the macrophages was then examined by harvesting cells from IPNs after 3 and 6 days of culture, and analyzing the expression of different surface markers. M0 and M2c macrophages seeded in IPNs as mono-cultures (MC) were analyzed as controls. The expression of CD45, a hematopoietic cell marker, was used to define the population of macrophages and differentiate them from the tumor cells within the co-cultures (CC). The initial phenotype of M0 and M2c macrophages was assessed before seeding the IPNs (Fig S4).

When originally M0 macrophages (CD45+/CD163−) were co-cultured with tumor cells at high stiffness (310 Pa), a small percentage of cells ultimately expressed the CCR7 receptor (M1 marker). In contrast, a significant increase was observed in the percentage of cells

expressing M2 markers (CD206 and CD163) when co-cultured with tumor cells after 3 and 6 days (Fig 4A). When M2c macrophages (CD45+/CD163+) were co-cultured with tumor cells, a significant subset (~20%) subsequently expressed the M1 marker CCR7 after 3 and 6 days. The percentage of cells expressing the M2a marker CD206 was only increased after 3 days in culture. Interestingly, the percentage of cells expressing the M2c marker CD163 decreased significantly in mono-cultures, to 20 and 10% at days 3 and 6, but remained around 50% in the co-cultures with tumor cells in IPNs, after 6 days of culture (Fig 4B).

Changes in the expression of macrophage surface markers were also analyzed in IPNs of low stiffness. However, matrix stiffness did not seem to have a strong effect on shaping the phenotype of originally M0 and M2c macrophages in this model (Fig 4 C–D).

3.5. Matrix stiffness and M2c macrophages jointly modulate the expression of specific EMT-related genes in A549 cell clusters

The next experiment evaluated if the co-culture of tumor cells with macrophages of different phenotypes, together with the matrix stiffness, could regulate the EMT process. A549 tumor cells were co-cultured (CC) with either M0 or M2c macrophages, in IPNs of low (30 Pa) and high (310 Pa) stiffness, for 3 and 6 days. Mono-cultures (MC) of A549 cells, seeded in IPNs of 30 and 310 Pa, were used as controls.

Vimentin expression (*VIM*), a mesenchymal marker typically upregulated in cells undergoing EMT [47], increased after 3 and 6 days of culture, when tumor cells were co-cultured with macrophages, irrespective of the initial macrophage phenotype (Fig 5A and S5A). A marked effect of the stiffness was also observed in both tumor cell mono-cultures and co-cultures, as upregulation of *VIM* was more pronounced at high stiffness (310 Pa). In M2c cultures, the upregulation of *VIM* was only observed in the co-cultures at high stiffness (310 Pa), irrespective of the time (Fig 5A).

The expression of E-Cadherin (*CDH1*), an epithelial marker critical for cell adhesion and downregulated during EMT [48], was influenced by both the phenotype of the macrophages and the stiffness (Fig 5B and S5B). *CDH1* was downregulated when tumor cells were co-cultured with M2c macrophages (Fig 5B), but not with M0 macrophages (Fig S5B). Moreover, a further reduction in the expression of *CDH1* was observed when tumor cells and M2c macrophages were cultured in an IPN of high stiffness. This reduction was also observed after 6 days in culture. (Fig 5B).

The expression of *PD-L1*, an immune checkpoint molecule recently related to the EMT process in different types of cancer [49–51], was only upregulated in tumor cells growing with initially M2c macrophages, in a stiffness dependent manner, after 3 days of culture. These effects were also observed after 6 days in co-culture at high stiffness (Fig 5C).

To further validate the gene expression results, protein expression for Vimentin, E-cadherin, and PD-L1 was analyzed by immunofluorescence in M0 and M2c co-cultures (CC). Alterations of the protein levels of these EMT markers were in general agreement with the findings of qPCR analysis of M0 (Fig S5) and M2c co-cultures (Fig 5) after 3 days and 6 days in culture. An increase in the expression levels in cells staining positive for Vimentin

was observed regardless of the initial macrophage phenotype after 3 days (Fig 5D and S5D), but was only observed in M2c co-cultures after 6 days. In contrast, a decrease in the expression levels of E-cadherin was observed only when tumor cells were co-cultured with M2c macrophages. This downregulation was slightly observed after 6 days in culture (Fig 5D). PD-L1 expression levels were increased in both M0 and M2c co-cultures in a stiffness dependent manner after 3, and especially after 6 days in M2c co-cultures (Fig 5D).

4. Discussion

We utilized a hydrogel system of varying stiffness for co-culture of tumor cells and macrophages, to determine their influence on the EMT process. The first set of studies, examining the impact of stiffness in the absence of macrophages, demonstrated that changes in ECM stiffness enhance proliferation and the invasive phenotype of A549 lung adenocarcinoma cells. A particular range of stiffness (30-310 Pa that translate to ~ 0.1-1 kPa Young's modulus) was selected as it is relevant to the transition from healthy to malignant lung tissue [52,53]. Normal human lung parenchyma elastic modulus has been measured at 0.44 to 7.5 kPa, depending on the region [54,55]. According to this, stiffness could be further increased by modifying the polymer concentration, molecular weight and calcium concentration, to explore the effects of a greater range in future studies. In contrast to previous models [56,57,36,37], this approach allowed us to evaluate matrix stiffness itself as a biophysical regulator of the cell phenotype, without affecting pore structure or matrix composition. These findings agree with previous results using this model to evaluate the induction of a malignant phenotype in normal mammary epithelium [44].

Conditioned media from macrophages of different phenotypes modified tumor cell growth only in IPNs of high stiffness. M0 conditioned medium inhibited cell proliferation whereas M2c macrophages medium enhanced it, and modulated the expression of EMT-related genes in IPNs of high stiffness. Cell cluster area analysis, as a proxy for cell growth, showed that conditioned media from M0 and M2c macrophages have differential effects on tumor cells growing in IPNs of high stiffness. Invasiveness, as shown by cell cluster circularity, was mainly affected by matrix stiffness, regardless the type of conditioned media (Fig S3). Moreover, the analysis of EMT-related genes confirmed that the effect of the conditioned media was dependent on the matrix stiffness. At low stiffness, changes in the expression of EMT-related genes were not observed regardless of the macrophages conditioned media. On the other hand, at high stiffness, treatment with M2c conditioned media upregulated genes involved in proliferation and invasiveness (*CDH2*, *MYC* and *TWIST1*). These results suggest that in comparison to M0 macrophages, soluble cues secreted by M2c macrophages, significantly contribute together with matrix stiffness, to the development of a mesenchymal phenotype, promoting the metastatic process. Previous in vitro studies have shown that tumor-infiltrating cells such as lymphocytes and TAMs, produce a myriad of signaling molecules and cytokines that promote tumor development and progression [58–61]; however, these studies did not consider the impact of the surrounding matrix stiffness.

Co-culture with tumor cells induced the alternative activation of M0 macrophages towards an M2-like phenotype, independently of the matrix stiffness. This polarization switch was not observed in macrophages growing in mono-culture, suggesting an activation mediated by

direct contact or factors secreted by the tumor cells. On the other hand, the expression of M2c markers strikingly decreased in the mono-cultures of initially M2c macrophages compared to the co-cultures. It is important to highlight that not all the cells that were polarized prior seeding, assumed a M2c phenotype during the process (Fig S4). These results are consistent with previous observations in lung [62] and breast [16,63] cancer co-cultures with macrophages. A549 cells are also known to produce specific cytokines in vitro when co-cultured with macrophages that promote M2 polarization [62]. Although matrix stiffness did not shape macrophage phenotype in our studies, it has been reported that macrophages modify their adhesion properties and pro-inflammatory cytokine release profile when cultured on stiff substrates [64–66].

M2c polarized macrophages, when present in co-culture, jointly contributed with ECM stiffness to regulate the expression of EMT markers. Co-culturing originally M0 or M2c macrophages with tumor cells induced differential expression of EMT-related genes, but changes were stiffness-dependent and mostly appreciated in M2c co-cultures up to 6 days. Previous studies have shown that interactions with macrophages can enhance invasiveness, chemoresistance, and alter gene expression profiles in lung cancer cell lines in co-culture [45,67]. Indeed, certain macrophages phenotypes secrete different enzymes such as matrix-metalloproteinases (MMPs) capable of degrading the ECM, altering stiffness and composition, allowing cells to spread and detach from the tumor [60,68,69]. Recently, spheres composed of tumor cells and macrophages were grown embedded in Matrigel to study macrophage-dependent tumor cell invasion; however, matrix stiffness or changes in the phenotype of macrophages were not investigated [70,71].

This study highlights the importance of both mechanical and soluble cues in tumor progression. Our findings demonstrate how the mechanical properties of the tumor microenvironment can affect tumor cell growth and EMT, while also impacting how tumor cells regulate and are affected by macrophages. Overall, this data supports the influence of matrix stiffness and macrophages phenotype in the behavior of tumor cells in three-dimensional matrix environments.

5. Conclusions

Altering matrix stiffness enhanced tumor cell growth and invasiveness in 3D culture of A549 lung adenocarcinoma cells. Treatment of tumor cell clusters growing in IPNs of high stiffness with conditioned media from macrophages of different phenotypes significantly affected growth of tumor cell clusters. Co-culture of tumor cells and M0 macrophages led to an alternative activated M2-like phenotype. Matrix stiffness and M2c tumor-associated macrophages jointly regulated the invasive potential of tumor cells in vitro. Altogether, these findings suggest that although matrix stiffness is considered a key factor in the induction of the EMT process, the contribution of other components of the TME such as tumor associated macrophages may be particularly relevant and therefore, should also be considered.

Supplementary Material

Refer to Web version on PubMed Central for supplementary material.

Acknowledgments

The authors would like to acknowledge the help of other members of the Mooney lab. The authors also thank Prof. María José Alonso (USC) for her support, Thomas Ferrante (Wyss Institute) for help with the cell cluster analysis, Patricia Viaño (University Clinical Hospital, Santiago de Compostela) for her technical support and sample processing, and Jose A. Diaz-Arias (University Clinical Hospital of Santiago de Compostela) for help/use the cytometer. The first author acknowledges a grant received from the Fundacion Barrie, Spain. The authors also acknowledge financial support given by the Carlos III Health Institute and the European Regional Development Fund (FEDER) (CP12/03150 and PI15/00828). Part of this work was also supported by the National Institute Of Dental & Craniofacial Research of the National Institutes of Health under Award Number 5R01DE013033 (DJM). The content is solely the responsibility of the authors and does not necessarily represent the official views of the National Institutes of Health.

References

1. Cassetta L, Cassol E, Poli G. Macrophage polarization in health and disease. Scientific World Journal. 2011; 11:2391–402. [PubMed: 22194670]
2. Sica A, Schioppa T, Mantovani A, Allavena P. Tumour-associated macrophages are a distinct M2 polarised population promoting tumour progression: potential targets of anti-cancer therapy. Eur J Cancer. 2006; 42:717–27. [PubMed: 16520032]
3. Xing F, Saidou J, Watabe K. Cancer associated fibroblasts (CAFs) in tumor microenvironment. Front Biosci (Landmark Ed. 2010; 15:166–79. [PubMed: 20036813]
4. Pundavela J, Roselli S, Faulkner S, Attia J, Scott RJ, Thorne RF, Forbes JF, Bradshaw RA, Walker MM, Jobling P, Hondermarck H. Nerve fibers infiltrate the tumor microenvironment and are associated with nerve growth factor production and lymph node invasion in breast cancer. Mol Oncol. 2015; 9:1626–35. [PubMed: 26009480]
5. Rahir G, Moser M. Tumor microenvironment and lymphocyte infiltration. Cancer Immunol Immunother. 2012; 61:751–9. [PubMed: 22488275]
6. Lu P, Weaver VM, Werb Z. The extracellular matrix: a dynamic niche in cancer progression. J Cell Biol. 2012; 196:395–406. [PubMed: 22351925]
7. Herrmann D, Conway JRW, Vennin C, Magenau A, Hughes WG, Morton JP, Timpson P. Three-dimensional cancer models mimic cell-matrix interactions in the tumour microenvironment. Carcinogenesis. 2014; 35:1671–9. [PubMed: 24903340]
8. Butcher DT, Alliston T, Weaver VM. A tense situation: forcing tumour progression. Nat Rev Cancer. 2009; 9:108–22. [PubMed: 19165226]
9. Sinkus R, Lorenzen J, Schrader D, Lorenzen M, Dargatz M, Holz D. High-resolution tensor MR elastography for breast tumour detection. Phys Med Biol. 2000; 45:1649–64. [PubMed: 10870716]
10. Swaminathan V, Mythreye K, O'Brien ET, Berchuck A, Blobe GC, Superfine R. Mechanical stiffness grades metastatic potential in patient tumor cells and in cancer cell lines. Cancer Res. 2011; 71:5075–80. [PubMed: 21642375]
11. Mouw JK, Yui Y, Damiano L, Bainer RO, Lakins JN, Acerbi I, Ou G, Wijekoon AC, Levental KR, Gilbert PM, Hwang ES, Chen Y-Y, Weaver VM. Tissue mechanics modulate microRNA-dependent PTEN expression to regulate malignant progression. Nat Med. 2014; 20:360–7. [PubMed: 24633304]
12. Branco da Cunha C, Klumpers DD, Li WA, Koshy ST, Weaver JC, Chaudhuri O, Granja PL, Mooney DJ. Influence of the stiffness of three-dimensional alginate/collagen-I interpenetrating networks on fibroblast biology. Biomaterials. 2014; 35:8927–36. [PubMed: 25047628]
13. Bin Kim J. Three-dimensional tissue culture models in cancer biology. Semin Cancer Biol. 2005; 15:365–77. [PubMed: 15975824]

14. Lech M, Anders H-J. Macrophages and fibrosis: How resident and infiltrating mononuclear phagocytes orchestrate all phases of tissue injury and repair. Biochim Biophys Acta. 2013; 1832:989–97. [PubMed: 23246690]
15. Clarke DL, Carruthers AM, Mustelin T, Murray LA. Matrix regulation of idiopathic pulmonary fibrosis: the role of enzymes. Fibrogenesis Tissue Repair. 2013; 6:20. [PubMed: 24279676]
16. Sousa S, Brion R, Lintunen M, Kronqvist P, Sandholm J, Mönkkönen J, Kellokumpu-Lehtinen P-L, Lauttia S, Tynninen O, Joensuu H, Heymann D, Määttä JA. Human breast cancer cells educate macrophages toward the M2 activation status. Breast Cancer Res. 2015; 17:101. [PubMed: 26243145]
17. Pollard JW. Tumour-educated macrophages promote tumour progression and metastasis. Nat Rev Cancer. 2004; 4:71–8. [PubMed: 14708027]
18. Leimgruber A, Berger C, Cortez-Retamozo V, Etzrodt M, Newton AP, Waterman P, Figueiredo JL, Kohler RH, Elpek N, Mempel TR, Swirski FK, Nahrendorf M, Weissleder R, Pittet MJ. Behavior of endogenous tumor-associated macrophages assessed in vivo using a functionalized nanoparticle. Neoplasia. 2009; 11:459–68. 2. following 468. [PubMed: 19412430]
19. Coffelt SB, Hughes R, Lewis CE. Tumor-associated macrophages: effectors of angiogenesis and tumor progression. Biochim Biophys Acta. 2009; 1796:11–8. [PubMed: 19269310]
20. Vasievich EA, Huang L. The suppressive tumor microenvironment: a challenge in cancer immunotherapy. Mol Pharm. 2011; 8:635–41. [PubMed: 21545153]
21. Mosser DM, Edwards JP. Exploring the full spectrum of macrophage activation. Nat Rev Immunol. 2008; 8:958–69. [PubMed: 19029990]
22. Solinas G, Schiarea S, Liguori M, Fabbri M, Pesce S, Zammataro L, Pasqualini F, Nebuloni M, Chiabrando C, Mantovani A, Allavena P. Tumor-conditioned macrophages secrete migration-stimulating factor: a new marker for M2-polarization, influencing tumor cell motility. J Immunol. 2010; 185:642–52. [PubMed: 20530259]
23. Solinas G, Germano G, Mantovani A, Allavena P. Tumor-associated macrophages (TAM) as major players of the cancer-related inflammation. J Leukoc Biol. 2009; 86:1065–73. [PubMed: 19741157]
24. S B Jr, Carron E, Vallespinós M, Machado HL. Cancer Stem Cells and Macrophages: Implications in Tumor Biology and Therapeutic Strategies. Mediators Inflamm. 2015; 2016
25. Mantovani A, Locati M. Tumor-associated macrophages as a paradigm of macrophage plasticity, diversity, and polarization: lessons and open questions. Arterioscler Thromb Vasc Biol. 2013; 33:1478–83. [PubMed: 23766387]
26. Mantovani A, Sica A, Sozzani S, Allavena P, Vecchi A, Locati M. The chemokine system in diverse forms of macrophage activation and polarization. Trends Immunol. 2004; 25:677–86. [PubMed: 15530839]
27. Rőszer T. Understanding the Mysterious M2 Macrophage through Activation Markers and Effector Mechanisms. Mediators Inflamm. 2015; 2015:816460. [PubMed: 26089604]
28. Fischbach C, Chen R, Matsumoto T, Schmelzle T, Brugge JS, Polverini PJ, Mooney DJ. Engineering tumors with 3D scaffolds. Nat Methods. 2007; 4:855–60. [PubMed: 17767164]
29. Infanger DW, Lynch ME, Fischbach C. Engineered culture models for studies of tumor-microenvironment interactions. Annu Rev Biomed Eng. 2013; 15:29–53. [PubMed: 23642249]
30. Geckil H, Xu F, Zhang X, Moon S, Demirci U. Engineering hydrogels as extracellular matrix mimics. Nanomedicine (Lond). 2010; 5:469–84. [PubMed: 20394538]
31. Tong X, Yang F. Engineering interpenetrating network hydrogels as biomimetic cell niche with independently tunable biochemical and mechanical properties. Biomaterials. 2014; 35:1807–15. [PubMed: 24331710]
32. Song H-HG, Park KM, Gerecht S. Hydrogels to model 3D in vitro microenvironment of tumor vascularization. Adv Drug Deliv Rev. 2014; 79-80:19–29. [PubMed: 24969477]
33. Szot CS, Buchanan CF, Freeman JW, Rylander MN. 3D in vitro bioengineered tumors based on collagen I hydrogels. Biomaterials. 2011; 32:7905–12. [PubMed: 21782234]
34. Zhu J, Marchant RE. Design properties of hydrogel tissue-engineering scaffolds. Expert Rev Med Devices. 2011; 8:607–26. [PubMed: 22026626]

35. Raeber GP, Lutolf MP, Hubbell JA. Molecularly engineered PEG hydrogels: a novel model system for proteolytically mediated cell migration. Biophys J. 2005; 89:1374–88. [PubMed: 15923238]
36. Cramer GM, Jones DP, El-Hamidi H, Celli JP. ECM Composition and Rheology Regulate Growth, Motility, and Response to Photodynamic Therapy in 3D Models of Pancreatic Ductal Adenocarcinoma Gwendolyn. Mol Cancer Res. 15:15–25.
37. Nguyen-Ngoc K-V, Cheung KJ, Brenot A, Shamir ER, Gray RS, Hines WC, Yaswen P, Werb Z, Ewald AJ. ECM microenvironment regulates collective migration and local dissemination in normal and malignant mammary epithelium.
38. Kraning-Rush CM, Reinhart-King CA. Controlling matrix stiffness and topography for the study of tumor cell migration. Cell Adhes Migr. 2012; 6:274–9.
39. Hagemann T, Wilson J, Kulbe H, Li NF, Leinster DA, Charles K, Klemm F, Pukrop T, Binder C, Balkwill FR. Macrophages Induce Invasiveness of Epithelial Cancer Cells Via NF-B and JNK. J Immunol. 2005; 175:1197–205. [PubMed: 16002723]
40. Wang R, Zhang J, Chen S, Lu M, Luo X, Yao S, Liu S, Qin Y, Chen H. Tumor-associated macrophages provide a suitable microenvironment for non-small lung cancer invasion and progression. Lung Cancer. 2011; 74:188–96. [PubMed: 21601305]
41. Liu C-Y, Xu J-Y, Shi X-Y, Huang W, Ruan T-Y, Xie P, Ding J-L. M2-polarized tumor-associated macrophages promoted epithelial-mesenchymal transition in pancreatic cancer cells, partially through TLR4/IL-10 signaling pathway. Lab Invest. 2013; 93:844–54. [PubMed: 23752129]
42. Dehai C, Bo P, Qiang T, Lihua S, Fang L, Shi J, Jingyan C, Yan Y, Guangbin W, Zhenjun Y. Enhanced invasion of lung adenocarcinoma cells after co-culture with THP-1-derived macrophages via the induction of EMT by IL-6. Immunol Lett. 2014; 160:1–10. [PubMed: 24698728]
43. Schmall A, Al-Tamari HM, Herold S, Kampschulte M, Weigert A, Wietelmann A, Vipotnik N, Grimminger F, Seeger W, Pullamsetti SS, Savai R. Macrophage and Cancer Cell Crosstalk via CCR2 and CX3CR1 is a Fundamental Mechanism Driving Lung Cancer. Am J Respir Crit Care Med. 2015; 191:437–47. [PubMed: 25536148]
44. Chaudhuri O, Koshy ST, Branco da Cunha C, Shin J-W, Verbeke CS, Allison KH, Mooney DJ. Extracellular matrix stiffness and composition jointly regulate the induction of malignant phenotypes in mammary epithelium. Nat Mater. 2014; 13:970–8. [PubMed: 24930031]
45. Genin M, Clement F, Fattaccioli A, Raes M, Michiels C. M1 and M2 macrophages derived from THP-1 cells differentially modulate the response of cancer cells to etoposide. BMC Cancer. 2015; 15:577. [PubMed: 26253167]
46. Levental KR, Yu H, Kass L, Lakins JN, Egeblad M, Erler JT, Fong SFT, Csiszar K, Giaccia A, Weninger W, Yamauchi M, Gasser DL, Weaver VM. Matrix crosslinking forces tumor progression by enhancing integrin signaling. Cell. 2009; 139:891–906. [PubMed: 19931152]
47. Liu C, Lin H-H, Tang M, Wang Y-K. Vimentin contributes to epithelial-mesenchymal transition cancer cell mechanics by mediating cytoskeletal organization and focal adhesion maturation. Oncotarget. 2015; 6:15966–83. [PubMed: 25965826]
48. Gheldof A, Berx G. Cadherins and epithelial-to-mesenchymal transition. Prog Mol Biol Transl Sci. 2013; 116:317–36. [PubMed: 23481201]
49. Ritprajak P, Azuma M. Intrinsic and extrinsic control of expression of the immunoregulatory molecule PD-L1 in epithelial cells and squamous cell carcinoma. Oral Oncol. 2015; 51:221–8. [PubMed: 25500094]
50. Tsutsumi S, Saeki H, Nakashima Y, Ito S, Oki E, Morita M, Oda Y, Okano S, Maehara Y. Programmed death-ligand 1 expression at tumor invasive front is associated with epithelial-mesenchymal transition and poor prognosis in esophageal squamous cell carcinoma. Cancer Sci. 2017; 108:1119–27. [PubMed: 28294486]
51. Ock C-Y, Kim S, Keam B, Kim M, Kim TM, Kim J-H, Jeon YK, Lee J-S, Kwon SK, Hah JH, Kwon T-K, Kim D-W, Wu H-G, Sung M-W, Heo DS. PD-L1 expression is associated with epithelial-mesenchymal transition in head and neck squamous cell carcinoma. Oncotarget. 2016; 7:15901–14. [PubMed: 26893364]
52. Butcher DT, Alliston T, Weaver VM. A tense situation: forcing tumour progression. Nat Rev Cancer. 2009; 9:108–22. [PubMed: 19165226]

53. Cox TR, Erler JT. Remodeling and homeostasis of the extracellular matrix: implications for fibrotic diseases and cancer. Dis Model Mech. 2011; 4:165–78. [PubMed: 21324931]
54. White ES. Lung extracellular matrix and fibroblast function. Ann Am Thorac Soc. 2015; 12(Suppl 1):S30–3. [PubMed: 25830832]
55. Booth AJ, Hadley R, Cornett AM, Dreffs AA, Matthes SA, Tsui JL, Weiss K, Horowitz JC, Fiore VF, Barker TH, Moore BB, Martinez FJ, Niklason LE, White ES. Acellular normal and fibrotic human lung matrices as a culture system for in vitro investigation. Am J Respir Crit Care Med. 2012; 186:866–76. [PubMed: 22936357]
56. Paszek MJ, Zahir N, Johnson KR, Lakins JN, Rozenberg GI, Gefen A, Reinhart-King CA, Margulies SS, Dembo M, Boettiger D, Hammer DA, Weaver VM. Tensional homeostasis and the malignant phenotype. Cancer Cell. 2005; 8:241–54. [PubMed: 16169468]
57. Provenzano PP, Inman DR, Eliceiri KW, Keely PJ. Matrix density-induced mechanoregulation of breast cell phenotype, signaling and gene expression through a FAK-ERK linkage. Oncogene. 2009; 28:4326–43. [PubMed: 19826415]
58. Alonso-Nocelo M, Abuín C, López-López R, de la Fuente M, de la Fuente M. Development and characterization of a three-dimensional co-culture model of tumor T cell infiltration. Biofabrication. 2016; 8:25002.
59. Croci DO, Zacarías Fluck MF, Rico MJ, Matar P, Rabinovich GA, Scharovsky OG. Dynamic cross-talk between tumor and immune cells in orchestrating the immunosuppressive network at the tumor microenvironment. Cancer Immunol Immunother. 2007; 56:1687–700. [PubMed: 17571260]
60. Mohamed MM, El-Ghonaimy EA, Nouh MA, Schneider RJ, Sloane BF, El-Shinawi M. Cytokines secreted by macrophages isolated from tumor microenvironment of inflammatory breast cancer patients possess chemotactic properties. Int J Biochem Cell Biol. 2014; 46:138–47. [PubMed: 24291763]
61. Engström A, Erlandsson A, Delbro D, Wijkander J. Conditioned media from macrophages of M1, but not M2 phenotype, inhibit the proliferation of the colon cancer cell lines HT-29 and CACO-2. Int J Oncol. 2014; 44:385–92. [PubMed: 24296981]
62. Müller-Quernheim UC, Potthast L, Müller-Quernheim J, Zissel G. Tumor-cell co-culture induced alternative activation of macrophages is modulated by interferons in vitro. J Interferon Cytokine Res. 2012; 32:169–77. [PubMed: 22280057]
63. Hollmén M, Roudnicky F, Karaman S, Detmar M. Characterization of macrophage - cancer cell crosstalk in estrogen receptor positive and triple-negative breast cancer. Sci Rep. 2015; 5:1–10.
64. Blakney AK, Swartzlander MD, Bryant SJ. The effects of substrate stiffness on the in vitro activation of macrophages and in vivo host response to poly(ethylene glycol)-based hydrogels. J Biomed Mater Res A. 2012; 100:1375–86. [PubMed: 22407522]
65. Previtera ML, Sengupta A. Substrate Stiffness Regulates Proinflammatory Mediator Production through TLR4 Activity in Macrophages. PLoS One. 2015; 10:e0145813. [PubMed: 26710072]
66. Shukla VC, Higuita-Castro N, Nana-Sinkam P, Ghadiali SN. Substrate Stiffness Modulates Lung Cancer Cell Migration but not Epithelial to Mesenchymal Transition. J Biomed Mater Res A. 2016; 104:1182–93. [PubMed: 26779779]
67. Yuan A, Hsiao Y-J, Chen H-YH-W, Chen H-YH-W, Ho C-C, Chen Y-Y, Liu Y-C, Hong T-H, Yu S-L, Chen JJW, Yang P-C. Opposite Effects of M1 and M2 Macrophage Subtypes on Lung Cancer Progression. Sci Rep. 2015; 5:14273. [PubMed: 26399191]
68. Kessenbrock K, Plaks V, Werb Z. Matrix Metalloproteinases: Regulators of the Tumor Microenvironment. Cell. 2010; 141:52–67. [PubMed: 20371345]
69. Afik R, Zigmond E, Vugman M, Klepfish M, Shimshoni E, Pasmanik-Chor M, Shenoy A, Bassat E, Halpern Z, Geiger T, Sagi I, Varol C. Tumor macrophages are pivotal constructors of tumor collagenous matrix. J Exp Med. 2016 jem.20151193.
70. Guiet R, Van Goethem E, Cougoule C, Balor S, Valette A, Al Saati T, Lowell CA, Le Cabec V, Maridonneau-Parini I. The process of macrophage migration promotes matrix metalloproteinase-independent invasion by tumor cells. J Immunol. 2011; 187:3806–14. [PubMed: 21880978]
71. Dwyer AR, Ellies LG, Holme AL, Pixley FJ. A three-dimensional co-culture system to investigate macrophage-dependent tumor cell invasion. J Biol Methods. 2016; 3:e49.

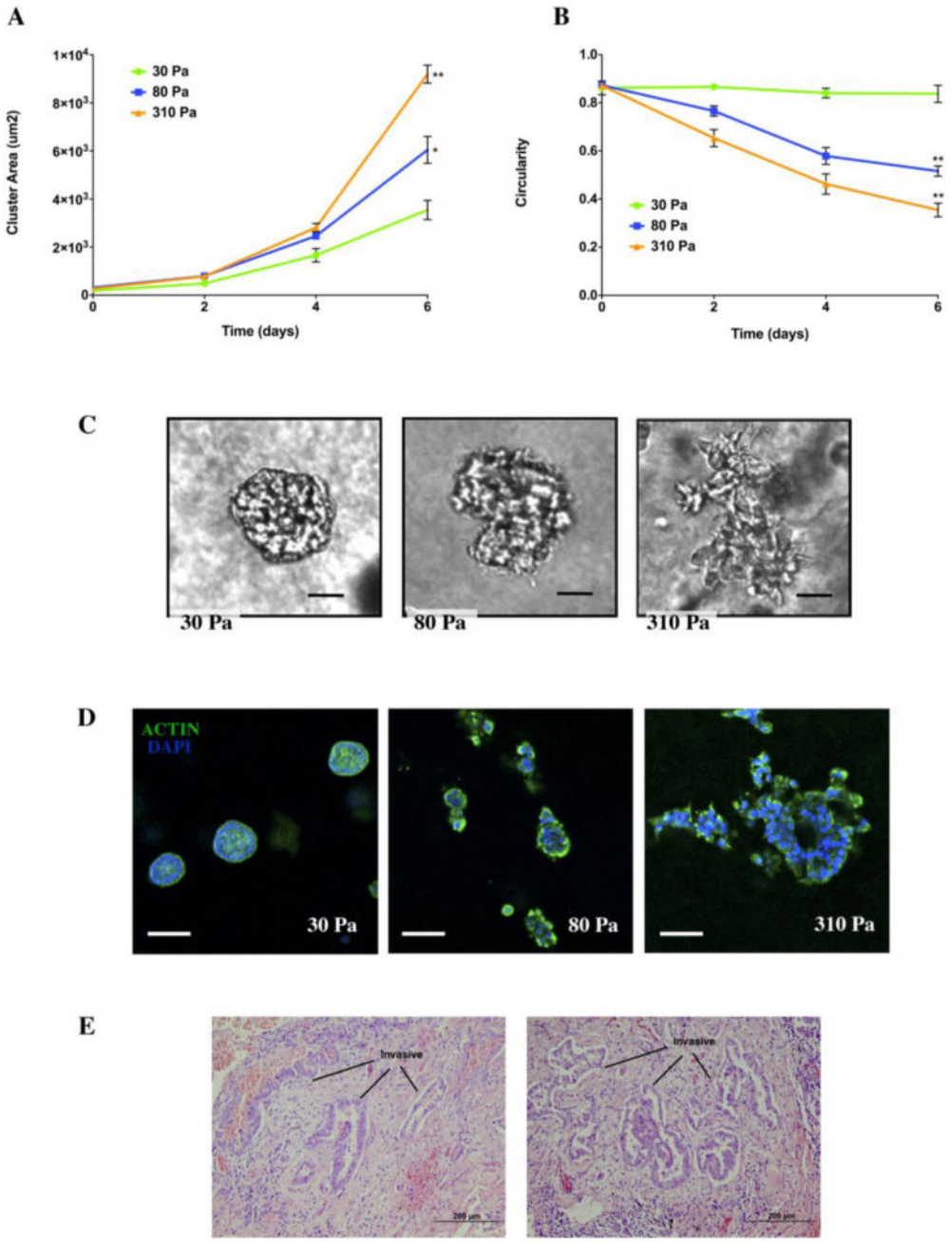

Figure 1. Increased stiffness of ECM enhances the growth and invasive phenotype in A549 cells

Quantification of **(A)** cluster area and (**B**) invasiveness of cell clusters, as a function of time and stiffness in cells encapsulated in hydrogels of low (30 Pa), intermediate (80 Pa) and high (310 Pa) stiffness. Data shown as mean ± SD. ** p value < 0.01, * p value < 0.05 compared to 30 Pa. **(C**) Bright-field images of A549 clusters in IPNs of the same stiffness at day 6. Scale bar 10 μm. (**D**) Confocal immunofluorescence imaging of F-Actin from cryosections of A549 clusters in IPNs with moduli of 30, 80 and 310 Pa at day 6. DAPI staining is in blue. Scale bar 50 μm. **E**) H&E staining of two human NSCLC adenocarcinoma lung tissue samples. Invasive glands are indicated.

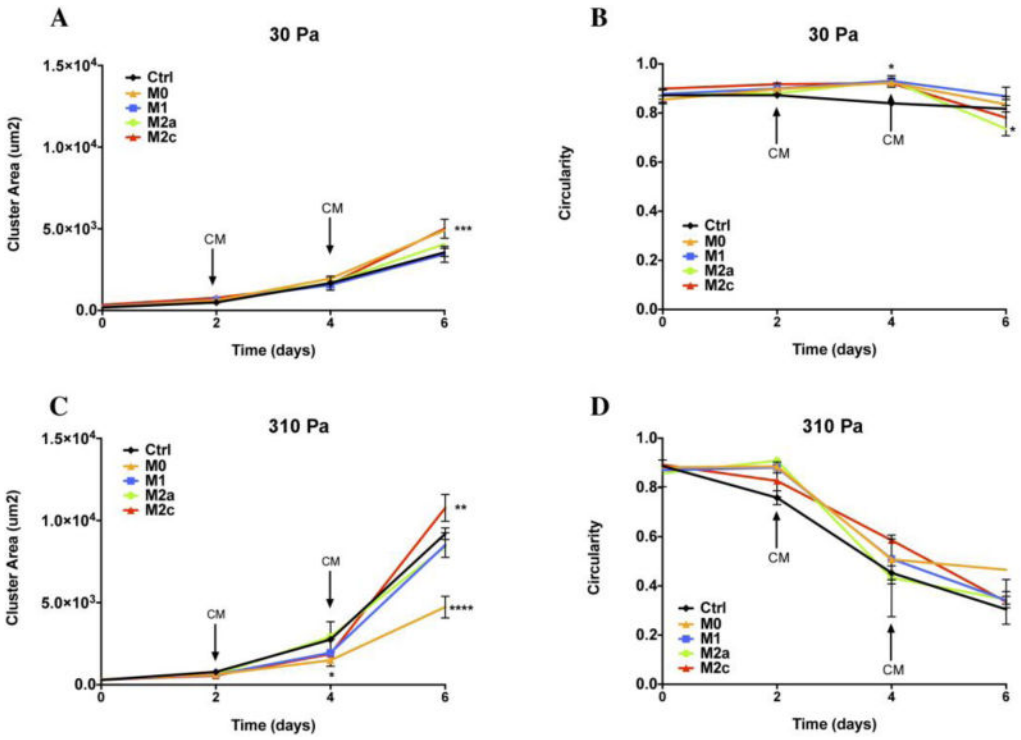

Figure 2. Conditioned medium (CM) from different macrophages phenotypes modifies tumor cell growth in IPNs of high stiffness

Quantification of cluster area (**A** and **C**) and circularity (**B** and **D**) of A549 cell clusters treated with control and macrophages conditioned media (CM) from cultures of different macrophage subtypes (M0, M1, M2a and M2c), as a function of stiffness (30 and 310 Pa) and time. Times at which CM was added to A549 cultures is indicated with arrows. Data shown as mean ± SD. **** p value <0.0001, ** p value < 0.01, * p value < 0.05 compared to control medium (Ctrl).

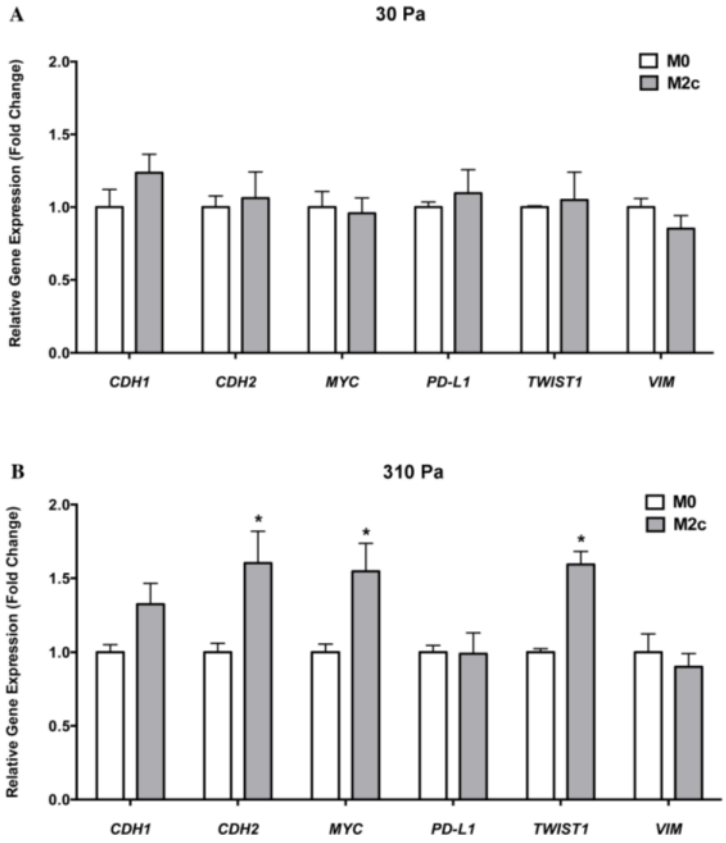

Figure 3. Higher stiffness maintains tumorigenic phenotype in the presence of M2c CM, by increasing expression of genes associated with EMT

Relative gene expression of A549 tumor mono-cultures in (**A**) 30 Pa (low) and (**B**) 310 Pa (high) stiffness IPNs treated with conditioned media (CM) from M0 and M2c macrophages. CM was added at days 2 and 4 of culture. Gene expression analyzed at day 6. All data are shown as mean ± SD. *$p < 0.05$ compared to M0 CM.

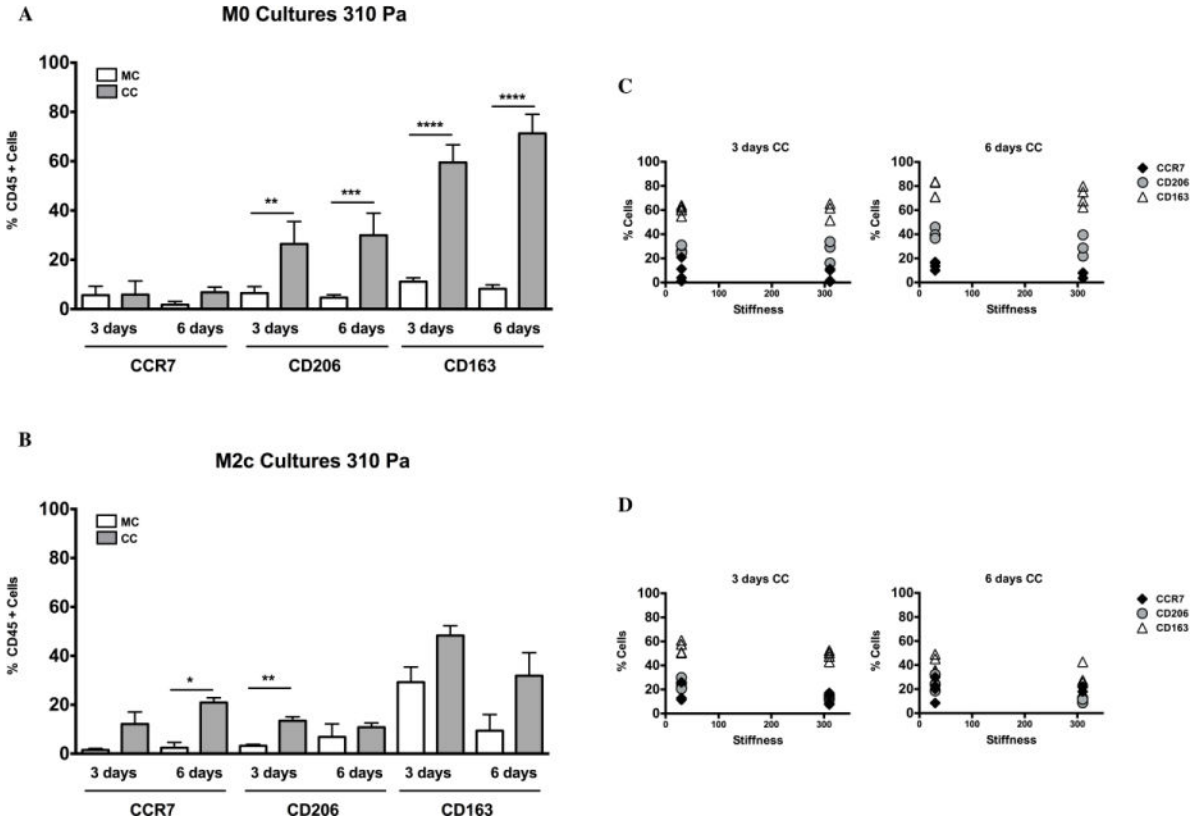

Figure 4. Co-culture with tumor cells induces the polarization of M0 macrophages towards an M2-like phenotype

Macrophages were harvested from M0 (**A–C**) and M2c (**B–D**) mono-cultures (MC) and co-cultures (CC) with tumor cells. Cells were harvested and analyzed at day 3 and 6. Changes in cell surface marker expression in the various conditions were determined by flow cytometry analysis. The percentage of CD45+ cells expressing CCR7+ (M1 marker), CD206+ (M2a marker), and CD163+ (M2c marker) is shown as mean ± SD. (****$p < 0.0001$; ***$p < 0.001$; **$p < 0.01$; *$p < 0.05$). (**C–D**) Scatter plots show individual data points representing the percentage of CD45+ cells (CCR7, CD206 and CD163 +) as a function of stiffness.

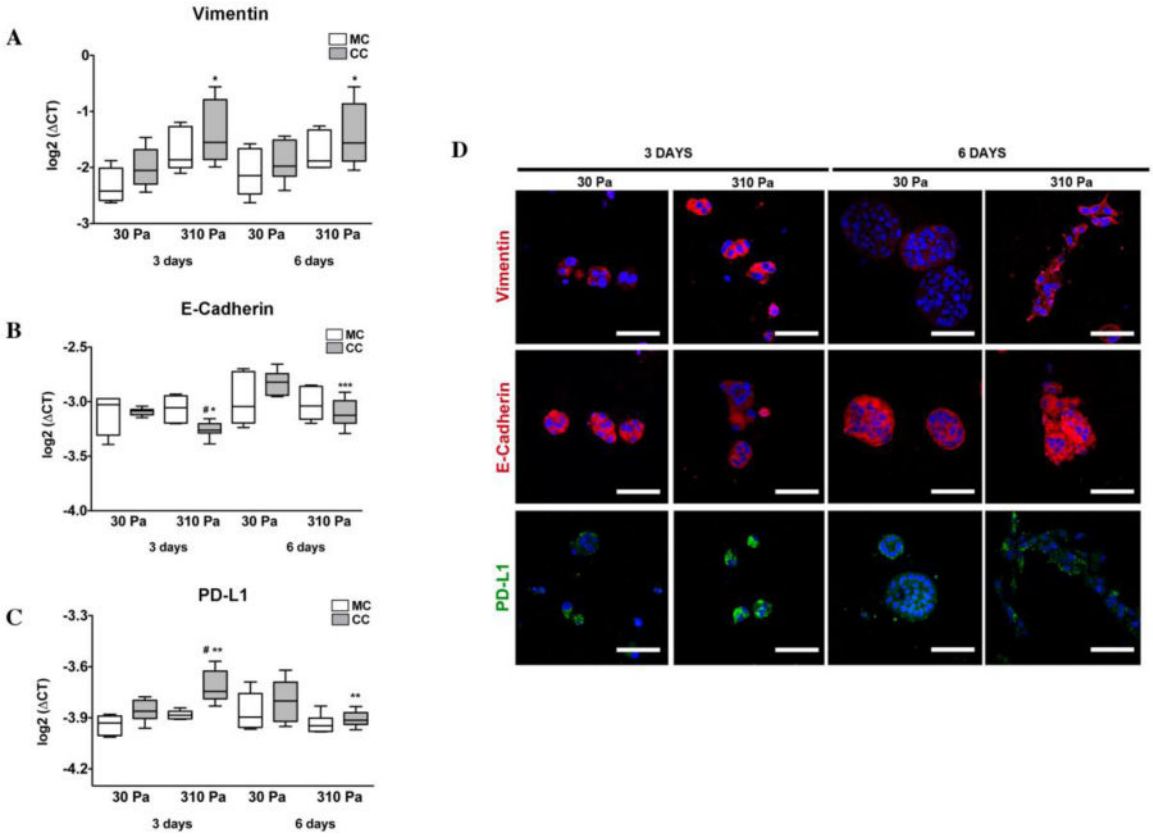

Figure 5. Matrix stiffness and M2c macrophages jointly regulate the expression of EMT-related genes

Relative gene expression of Vimentin (**A**), E-cadherin (**B**) and PD-L1 (**C**) in tumor cells mono-cultures (MC) and co-cultures (CC) of tumor cells with initially M2c macrophages, growing in IPNs of low (30 Pa) and high (310 Pa) stiffness after 3 and 6 days. Statistically significant differences are noted (*** p value < 0.001**; p value < 0.01; * p value < 0.05 compared to 30 Pa, # compared to mono-cultures (MC). (**D**) Representative micrographs of confocal immunofluorescence imaging of EMT-related markers Vimentin, E-Cadherin and PD-L1 in cross-sections of co-cultures (CC) of tumor cells and M2c macrophages, in IPNs of low (30 Pa) and high (310 Pa) stiffness after 3 and 6 days. DAPI staining is shown in blue. Scale bars are 50 μm.